X-Ray and Neutron Diffraction with Amorphous $Ti_{67}Si_{33}$, $V_{67}Si_{33}$, and $Cr_{67}Si_{33}$

A. Präffcke, P. Lamparter, and S. Steeb

Max-Planck-Institut für Metallforschung, Institut für Werkstoffwissenschaft, Stuttgart, Germany

Z. Naturforsch. **48a**, 777–783 (1993); received April 13, 1993

The amorphous alloys $Ti_{67}Si_{33}$, $V_{67}Si_{33}$, and $Cr_{67}Si_{33}$ were produced by sputtering. Their structure was investigated by X-ray and neutron diffraction. X-ray diffraction showed that the structure of the three metallic glasses is not isomorphous. Neutron diffraction showed that Si–Si atomic pairs occur preferentially with distances distinctly larger than the atomic diameter of the Si atoms. For $T_{67}Si_{33}$ partial pair correlation functions could be evaluated from combination of the X-ray and the neutron data.

The structural results are compared with the structure of amorphous $Mn_{74}Si_{23}P_3$.

1. Introduction

Amorphous transition metal-metalloid alloys have been investigated extensively in the past [1]. Most of them were produced at eutectic compositions by rapid quenching of the melt. The silicides M_5Si_3 (M = Ti, V, Cr) have very high melting temperatures. Therefore, in the present work rf-sputtering was applied to produce the amorphous samples.

For the evaluation of partial structure factors and partial pair correlation functions from measured total functions different contrast variation techniques can be applied. One of them is the isomorphous substitution technique, where an element in an alloy is substituted by a chemically related one, which does not cause a change of the structure, but which has a different scattering length. The metals Ti, V, and Cr seemed to be suitable for this purpose because they are neighbours in the periodic table and their neutron scattering lengths are very different (negative for Ti, close to zero for V, and positive for Cr). A further technique is the combination of X-ray and neutron diffraction which provides very strong contrast in those cases where elements with a negative or zero neutron scattering length are involved. In the present study both methods were applied with the aim to derive the partial pair correlation functions of amorphous M_5Si_3.

Structural data for amorphous $Mn_{74}Si_{23}P_3$ from a previous study [2] are included for comparison.

Reprint requests to Dr. P. Lamparter, Max-Planck-Institut für Metallforschung, Institut für Werkstoffwissenschaft, Seestraße 92, 70174 Stuttgart, FRG.

2. Theoretical

In this section a brief summary of the symbols and relations as used in the present work is given. For a more detailed description see e.g. [1].

From the coherently scattered intensity per atom $I_c(Q)$ the total structure factor $S(Q)$ is obtained according to the Faber-Ziman notation [3]:

$$S(Q) = \frac{I_c(Q) - [\langle b^2\rangle - \langle b\rangle^2]}{\langle b\rangle^2}. \tag{1}$$

For a binary alloy it is a sum of three weighted partial structure factors $S_{ij}(Q)$:

$$S(Q) = \frac{c_1^2 b_1^2}{\langle b\rangle^2} S_{11}(Q) + \frac{c_2^2 b_2^2}{\langle b\rangle^2} S_{22}(Q) + 2\frac{c_1 c_2 b_1 b_2}{\langle b\rangle^2} S_{12}(Q), \tag{2}$$

where the symbols in (1) and (2) are:

$Q = \frac{4\pi}{\lambda}\sin\Theta$ = modulus of the scattering vector,
2Θ = scattering angle,
λ = wavelength of the radiation,
$\langle b\rangle = c_1 b_1 + c_2 b_2$,
$\langle b^2\rangle = c_1 b_1^2 + c_2 b_2^2$,
b_i = scattering length of component i, depending on Q for X-rays,
c_i = atomic fraction of component i.

Fourier transformation of $S(Q)$ yields the associated pair correlation function $G(R)$ and the pair distribution function $g(R)$, which both contain the same physical information in a somewhat different presen-

0932-0784 / 93 / 0700-0777 $ 01.30/0. – Please order a reprint rather than making your own copy.

tation:

$$G(R) = 4\pi R \varrho_0 [g(R) - 1]$$

$$= \frac{2}{\pi} \int_0^\infty Q\,[S(Q) - 1] \sin(QR)\, \mathrm{d}Q\,, \qquad (3)$$

where R = atomic distance, ϱ_0 = mean atomic number density.

Within the R-range below the distances of nearest neighbours $g(R)=0$ and $G(R)=-4\pi R\varrho_0$. The total functions in R-space are composed of the corresponding partial functions $G_{ij}(R)$ and $g_{ij}(R)$, respectively, with the same weighting factors W_{ij} as given in (2) for the structure factors.

$\varrho_{ij}(R) = c_j \varrho_0 g_{ij}(R)$ represents the number of j-type atoms per unit volume at distance R from a central i-type atom. The corresponding partial coordination number N_{ij} is obtained from

$$N_{ij} = \int 4\pi R^2 \varrho_{ij}(R)\, \mathrm{d}R\,, \qquad (4)$$

where the integration is performed over the main maximum of the $\varrho_{ij}(R)$ function. For the necessary separation of the main maximum from the partly overlapping second peak Gaussian fitting is a useful method, which in the present study was applied to the distribution functions $g(R)$.

3. Experimental and Data Reduction

3.1. Specimen Preparation

The amorphous specimens were prepared by rf-sputtering. The sputtering targets were produced from the arc melted alloys with nominal composition M_5Si_3 (M = Ti, V, Cr). Aluminium foil was used as substrate, which was dissolved by caustic soda solution after the sputtering process to obtain free standing amorphous foils. The deposition rate was about 0.2 grams per day. Chemical analysis of the amorphous specimens yielded the final composition $M_{67}Si_{33}$.

3.2. X-ray Diffraction

The X-ray diffraction experiments were performed with a Siemens D 500 diffractometer in transmission mode using Mo-K_α radiation. The instrument was equipped with a primary monochromator, a vacuum sample chamber, and a position sensitive detector. The measured intensities were corrected for background scattering, absorption, polarization, and for Compton scattering. After conversion into absolute scattering units according to the Gingrich method [4], the structure factors were calculated from (1). The scattering lengths were taken from [5]. For smoothing of the experimental data a cubic splinefit algorithm was applied. Due to the lack of experimental data the densities were interpolated from those of the pure constituents. These values usually are somewhat smaller than the real values for metallic glasses.

3.3. Neutron Diffraction

The neutron diffraction experiments were performed at the Saphir reactor, PSI Villigen, Switzerland, using the DMC powder diffractometer. About 3 grams of the shredded amorphous material was put into a cylindrical vanadium container with 8 mm diameter, 4.5 cm height, and 13 μm wall thickness. With the wavelength $\lambda = 1.086$ Å a Q-range from 0.5 $Å^{-1}$ up to 10.7 $Å^{-1}$ could be covered.

The measured intensities were corrected for background scattering, for the contribution of the container, and for absorption using the Paalman-Pings method [6]. The correction for multiple scattering was done according to Sears [7], and that for inelastic scattering according to Placzek [8]. The conversion of the corrected intensities into absolute scattering units was carried out with the Krogh-Moe method [9]. The scattering lengths and absorption cross sections were taken from [10]. The experimental data were smoothed by cubic splinefit.

The scattering patterns of the Ti–Si and the V–Si samples revealed that these alloys contained hydrogen impurities: an incoherent scattering contribution of hydrogen, which is continuously decaying with increasing Q, was superimposed on the oscillating signal from the amorphous sample. The separation of this contribution was done by the Fourier filtering method. In the Fourier transform $g(R)$ of the intensity $I_c(Q)$ the hydrogen contribution occurs as a peak at R-values well below the atomc distances. Replacement of this peak by the theoretical value $g(R)=0$ and back-transformation into Q-space yielded the corrected $I_c(Q)$ [11].

4. Results and Discussion

4.1. Structure Factors

Figure 1 shows the total structure factors $S_x(Q)$ as obtained with X-rays, and Fig. 2 the $S_n(Q)$ as obtained

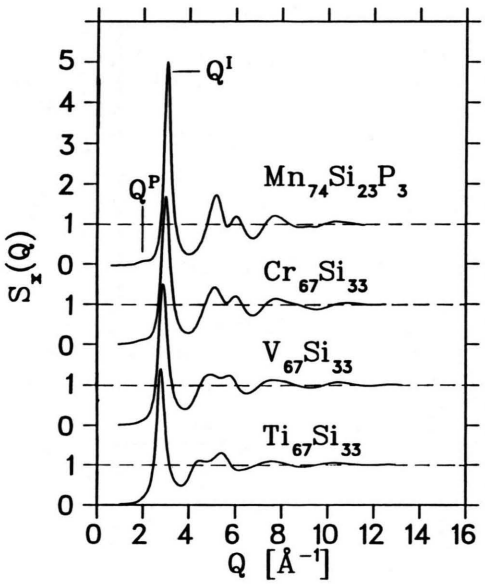

Fig. 1. Amorphous $M_{67}Si_{33}$ (M = Ti, V, Cr) and $Mn_{74}Si_{23}P_3$; X-ray diffraction: total structure factors $S_x(Q)$.

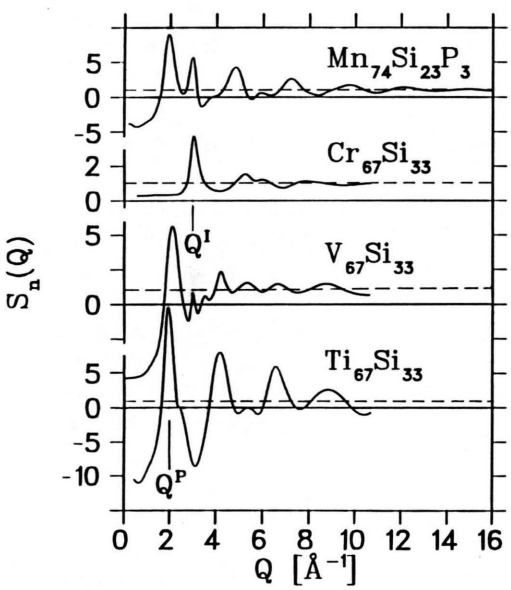

Fig. 2. Amorphous $M_{67}Si_{33}$ (M = Ti, V, Cr) and $Mn_{74}Si_{23}P_3$; neutron diffraction: total structure factors $S_n(Q)$.

with neutrons. The curves for $Mn_{74}Si_{23}P_3$ from [2], after renormalization according to the Faber-Ziman definition, are also shown for comparison. In Table 1 the weighting factors W_{ij} of the partial structure factors and of the partial pair correlation functions according to (2) are listed.

Table 1. Amorphous M–Si alloys (M = Ti, V, Cr, Mn): Weighting factors W_{ij} of the partial structure factors and correlation functions as given in (2).

		W_{MM}	W_{SiSi}	W_{MSi}
$Ti_{67}Si_{33}$	x	0.580	0.057	0.363
	n	6.09	2.16	−7.25
$V_{67}Si_{33}$	x	0.592	0.053	0.355
	n	0.05	1.51	−0.56
$Cr_{67}Si_{33}$	x	0.603	0.050	0.347
	n	0.410	0.130	0.461
$Mn_{74}Si_{23}P_3$	x	0.697	0.027	0.276
	n	2.79	0.45	−2.24

In the case of X-ray diffraction the weighting factors are almost the same for the three binary alloys. Thus, the total X-ray structure factors are expected to be the same if the three metallic glasses had the same structure, i.e. if the mutual substitution of the metal atoms Ti, V, and Cr were isomorphous. In fact, the general features of the total $S_x(Q)$ in Fig. 1 are quite similar for the three alloys: We observe a pronounced first maximum at Q^I, a second maximum, which shows a splitting up into two subpeaks, and further decaying oscillations. These general features are observed with most metallic glasses. However, there are also differences in the $S_x(Q)$ of the three alloys which reveal that we cannot treat them using the concept of isomorphous substitution between Ti, V, and Cr. First, the oscillations are shifted to larger Q-values in the series Ti–Si, V–Si, Cr–Si. This corresponds to the decrease of the Goldschmidt-diameter of the metal atom in the series $d_{Ti} = 2.94$ Å, $d_V = 2.72$ Å, $d_{Cr} = 2.56$ Å [12]. One might think of retaining the concept of isomorphous substitution, taking account of this size effect by rescaling the Q-scale in $S_x(Q)$, and accordingly the R-scale in $G_x(R)$, for the V–Si and the Cr–Si alloys to match the position of the first maximum of the Ti–Si alloy. However, a further substantial difference is observed in the range of the split second maximum. The ratio of the amplitudes of the two subpeaks becomes reversed in the series going from Ti via V to Cr. This implies that the deviation from isomorphous behaviour is more complicated than a simple size effect, but rather involves a difference in the atomic ordering effects. The $Mn_{74}Si_{23}P_3$ glass fits well into the series. Like $Cr_{67}Si_{33}$ it shows the indication of a subpeak at Q^P in front of the main maximum at Q^I. The splitting up of the second maximum where the first subpeak is the higher one is strongest for the Mn–Si–P glass.

The total neutron structure factors $S_n(Q)$ in Fig. 2 show large differences among each other, which are due to the fact that the weighting factors of the partial functions in Table 1 are very different. With the Cr–Si glass the W_{ij} are comparable to those for X-rays, and accordingly the neutron and X-ray $S(Q)$ are much alike, displaying the main maximum near $Q^I = 3.0$ Å^{-1}. With Ti–Si, V–Si, and Mn–Si–P this peak is strongly reduced, and the largest maximum occurs now at a distinctly smaller Q-value near $Q^P = 2$ Å^{-1}. From the weighting factors W_{ij} we conclude that this maximum is due to the Si–Si correlation. The position of Q^P, well below Q^I, implies that this correlation is characterized by Si–Si distances distinctly larger than the M–M as well as the M–Si nearest neighbour distances, i.e., the small Si atoms avoid to be in close contact in the amorphous structure. This structural behaviour has been found in all transition metal-metalloid glasses investigated up to now [1].

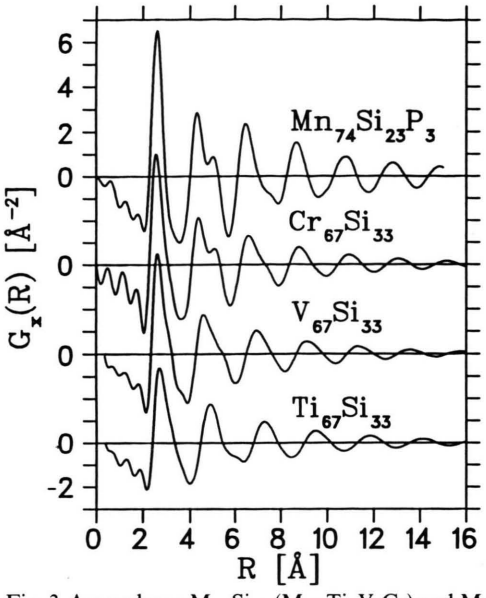

Fig. 3. Amorphous $M_{67}Si_{33}$ (M = Ti, V, Cr) and $Mn_{74}Si_{23}P_3$; X-ray diffraction: total pair correlation functions $G_x(R)$.

4.2. Pair Correlation Functions

Figure 3 shows the pair correlation functions $G_x(R)$ from X-ray diffraction. The radii of the first coordination shell R_x^I and the total coordination numbers N_x^I, calculated from $\varrho_x(R) = \varrho_0 g_x(R)$ according to (4), are listed in Table 2. The W_{ij} in Table 1 show that the $G_x(R)$ are composed mainly of $G_{MM}(R)$ and $G_{MSi}(R)$, whereas the contribution of $G_{SiSi}(R)$ is negligible. Thus the apparent radius R_x^I of the first coordination shell lies in between the M–M and the M–Si atomic distances. The shift of R_x^I to smaller values going from Ti–Si via V–Si to Cr–Si corresponds to the decrease of the Goldschmidt-diameter of the respective metal atom.

The non-isomorphous behaviour of the glasses, as stated before, is also displayed by the $G_x(R)$-functions: within the series $(Ti–V–Cr)_{67}Si_{33}$ the first maximum becomes higher and sharper, which is explained by the decreasing difference between the M–M and the M–Si atomic distances. However, the total coordination number N_x^I is the same within the experimental accuracy. The largest difference is found in the range of the split second maximum. The second subpeak occurs as a small bump for Ti, as a shoulder for V, and as a distinct subpeak for Cr, and it is shifted towards smaller R-values. The $Mn_{74}Si_{23}P_3$ alloy fits well into the series in Figure 3.

The pair correlation functions $G_n(R)$ derived from neutron diffraction are plotted in Figure 4. Their discussion in the following is based on the weighting factors W_{ij} in Table 1 and on the comparison with the $G_x(R)$ functions.

Table 2. Amorphous M–Si alloys (M = Ti, V, Cr, Mn): Structural parameters. R_x^I and N_x^I: radius and coordination number of first coordination shell from X-ray diffraction; R_{ij}: atomic distance of i–j pairs; $\Delta R_{ij}/R_{ij}$: distribution width; N_{ij}: coordination number of j-type atoms around i-type atoms; η_{SiM}: short range order parameter.

	$Ti_{67}Si_{33}$	$V_{67}Si_{33}$	$Cr_{67}Si_{33}$	$Mn_{74}Si_{23}P_3$
R_x^I [Å]	2.68	2.60	2.54	2.58
N_x^I	12.5	12.2	12.1	12.1
R_{MM} [Å]	3.02			2.66
$\Delta R_{MM}/R_{MM}$	0.25			0.17
N_{MM}	8.6			8.8
R_{MSi} [Å]	2.62			2.44
$\Delta R_{MSi}/R_{MSi}$	0.18			0.14
N_{MSi}	3.8			3.6
N_{SiM}	7.7			10.2
R_{SiSi} [Å]	2.1	3.1, 3.8		
N_{SiSi}	1	1.5, 6.0		
η_{SiM}	0.19			0.20–0.26

4.2.1 $Ti_{67}Si_{33}$

Due to the opposite signs of the scattering lengths of Ti ($b_{Ti} = -0.344 \cdot 10^{-12}$ cm) and Si ($b_{Si} = 0.415$

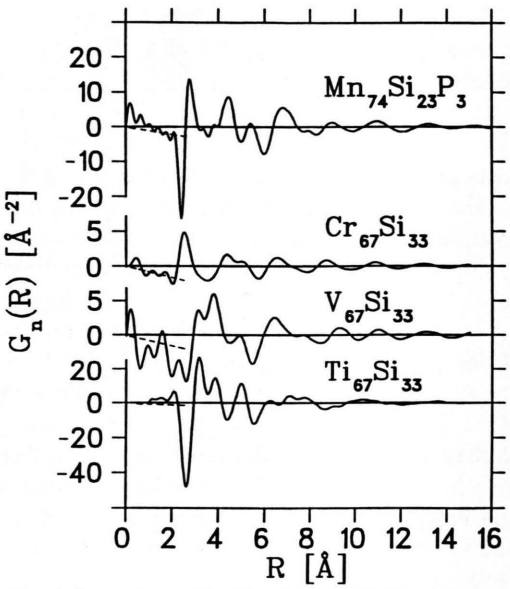

Fig. 4. Amorphous $M_{67}Si_{33}$ (M = Ti, V, Cr) and $Mn_{74}Si_{23}P_3$; neutron diffraction: total pair correlation functions $G_n(R)$. (– – –) $-4\pi R\varrho_0$.

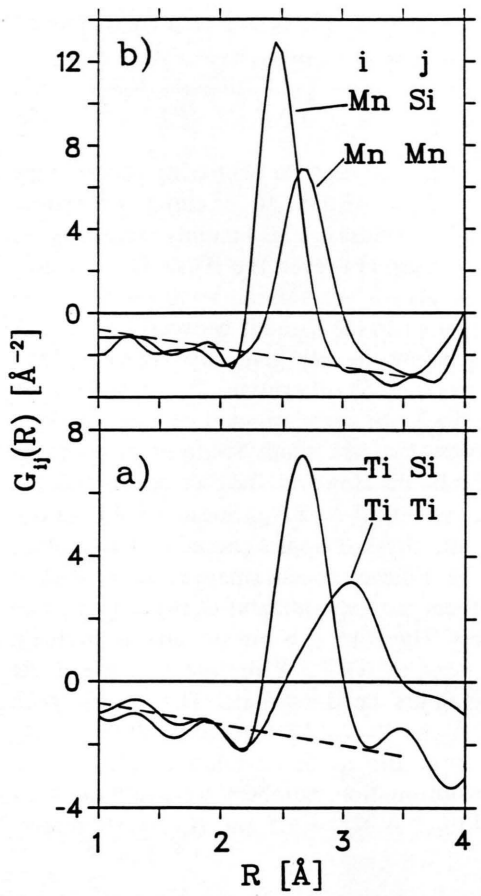

Fig. 5. a) Amorphous $Ti_{67}Si_{33}$, b) amorphous $Mn_{74}Si_{23}P_3$: partial pair correlation functions $G_{ij}(R)$.

$\cdot 10^{-12}$ cm) the partial Ti–Si correlation contributes with negative sign to the total $G_n(R)$ and is displayed in Fig. 4 as a strong negative peak. Then follows the Ti–Ti correlation as a positive peak.

In the case of neutron diffraction the contribution of the Si–Si correlation is not negligible. The small peak at $R = 2.1$ Å suggests some direct Si–Si neighbours. Fitting a Gaussian to this peak yields the coordination number $N_{SiSi} \approx 1$, which has to be considered as an estimation because of the influence of the partly overlapping negative Ti–Si contribution. As already mentioned, the Si–Si pairs are found preferably at larger distances. We attribute the peak at $R = 3.84$ Å to the Si–Si correlation. This is supported by the fact that the total X-ray function $G_x(R)$, where W_{SiSi} is very small, exhibits a minimum at this distance.

From $G_x(R)$ and $G_n(R)$ the partial pair correlation functions $G_{TiSi}(R)$ and $G_{TiTi}(R)$ were calculated within the range of the first coordination shell by solving the associated pair of equations according to (2). For $G_{SiSi}(R)$ the properly weighted Gaussian fit, as mentioned above, was inserted. The results are shown in Figure 5a. From the corresponding functions $g_{ij}(R)$ the atomic distances as the peak position, the bond length distribution widths as the full width at half maximum, and the coordination numbers from Gaussian fitting, were obtained and listed in Table 2. The Ti–Ti distance $R_{TiTi} = 3.02$ Å is slightly larger than the Goldschmidt diameter of the Ti atoms, $d_{Ti} = 2.94$ Å [12]. The apparent diameter of the Si atoms in the $Ti_{67}Si_{33}$ glass can be calculated as

$$d_{Si}^{a} = 2R_{TiSi} - R_{TiTi} = 2.22 \text{ Å}.$$

This value, distinctly smaller than the atomic diameter $d_{Si} = 2.43$ Å from [12], indicates the chemical interaction between the Si and the Ti atoms. The distribution of the bond length for the Ti–Si pairs is sharper, $\Delta R_{TiSi}/R_{TiSi} = 0.18$, than for the Ti–Ti pairs, $\Delta R_{TiTi}/R_{TiTi} = 0.25$, which gives further evidence of a chemical effect.

The short range order parameter according to the definition of Cargill and Spaepen [13] is calculated from the partial coordination numbers as $\eta_{SiTi} = 0.19$.

It is positive and thus reflects preferred heterocoordination in amorphous $Ti_{67}Si_{33}$.

4.2.2 $V_{67}Si_{33}$

Vanadium has a neutron scattering length very close to zero ($b_V = -0.038 \cdot 10^{-12}$ cm) and therefore $G_n(R)$ of the V–Si glass in Fig. 4 mainly represents the Si–Si correlations. However, the W_{ij} in Table 1 show that there is also a substantial V–Si contribution, which is negative. In the R-range between 2 Å and 3 Å $G_n(R)$ runs below the line given by $-4\pi R\varrho_0$, and according to (3) $g_n(R)$ is negative. This shows that in this range the V–Si correlations dominate and supports the view that the small Si-atoms avoid to be nearest neighbours. However, the oscillations of $G_n(R)$ around the theoretical $-4\pi R\varrho_0$ line at small R-values, which are non-physical ripples caused by termination effects in the Fourier transformation, show that at small distances the experimental $G_n(R)$ is influenced by this effect. Therefore it is not possible to decide if the small peak at $R = 2.3$ Å represents some direct Si–Si neighbours or is artificial. The double peak $R_{SiSi} = 3.1$ Å and $R_{SiSi} = 3.8$ Å represents the positive contribution of the Si–Si correlations. The corresponding coordination numbers were obtained by Gaussian fitting as $N_{SiSi} = 1.5$ and $N_{SiSi} = 6.0$, respectively.

4.2.3 $Cr_{67}Si_{33}$

The pair correlation function of $Cr_{67}Si_{33}$ in Fig. 4 is very similar to the corresponding function in Fig. 3 from X-ray diffraction. This is to be expected from the similar weighting factors in Table 1.

4.2.4 $Mn_{74}Si_{23}P_3$

The structural data of amorphous $Mn_{74}Si_{23}P_3$ were discussed in [2] in terms of density and concentration fluctuations according to Bhatia and Thornton [14]. In the present paper we consider atomic pairs (the P atoms were treated as Si atoms). With the assumption that within the range of the first coordination shell the contribution of Si–Si pairs is negligible, the partial pair correlation functions $G_{MnSi}(R)$ and $G_{MnMn}(R)$ and the related structural parameters were calculated from the combination of the X-ray and the neutron total $G(R)$ (see Fig. 5b and Table 2).

The Mn–Mn distance $R_{MnMn} = 2.66$ Å agrees with the Goldschmidt-diameter $d_{Mn} = 2.70$ Å. The apparent diameter of the Si atoms

$$d_{Si}^{a} = 2R_{MnSi} - R_{MnMn} = 2.22 \text{ Å}$$

is the same as in the case of the Ti–Si glass. Again the distribution of the bond length is sharper for the metal-metalloid pairs than for the metal-metal pairs.

The number of metal atoms around a metalloid atom in the Mn–Si–P glass, $N_{SiMn} = 10.2$, is higher than in the Ti–Si glass, $N_{SiTi} = 7.7$. This can be understood from the higher metal content and, in addition, from the smaller size of the Mn atoms compared with that of the Ti atoms.

With the assumption that the coordination number for direct Si–Si neighbours lies somewhere between zero and unity we obtain from the partial coordination numbers in Table 2 as an estimation for the short range order parameter

$$0.20 \leq \eta_{SiTi} \leq 0.26 ,$$

indicating preferred heterocoordination in amorphous $Mn_{74}Si_{23}P_3$. This behaviour has been also found in [2] on the basis of the Bhatia and Thornton approach.

5. Conclusions

Amorphous sputtered $M_{67}Si_{33}$ alloys (M = Ti, V, Cr) were investigated by X-ray and neutron diffraction. The structure of the three alloys is similar, but not fully isomorphous. Like in other metal-metalloid glasses nearest neighbour contact between the metalloid atoms is avoided. By combination of X-ray- and neutron diffraction-data for $Ti_{67}Si_{33}$ the partial Si–Ti and Ti–Ti correlation functions were determined. Their structural features are characterized by a chemical ordering effect in the amorphous alloy. Comparison with the amorphous alloy $Mn_{74}Si_{23}P_3$ shows similar structural properties.

Acknowledgement

Thanks are due to the Paul Scherrer Institute, Villingen, for allocation of beam time and to P. Fischer, PSI Villigen, for help during the neutron diffraction experiments.

[1] P. Lamparter and S. Steeb, in: Material Science and Technology, Vol. 1, Chapt. 4, pp. 217–288. VCH Publishers Inc., Weinheim 1993.
[2] G. Rainer-Harbach, P. Lamparter, F. Paasche, and S. Steeb, Proc. 4th Int. Conf. on Rapidly Quenched Metals (T. Masumoto and K. Suzuki, eds.), Japan Institute of Metals (1982), pp. 315–318.
[3] T. E. Faber and J. M. Ziman, Phil. Mag. **11,** 153 (1965).
[4] N. S. Gingrich, Rev. Mod. Phys. **15,** 90 (1943).
[5] J. H. Hubbell, W. J. Veigele, E. A. Briggs, R. T. Brown, D. T. Cromer, and R. J. Howeston, J. Phys. Chem. Rev. Data **4,** 471 (1975).
[6] H. H. Paalman and C. J. Pings, J. Appl. Phys. **33,** 2635 (1962).
[7] V. F. Sears, Adv. Phys. **24,** 1 (1975).
[8] G. Placzek, Phys. Rev. **31,** 377 (1952).
[9] J. Krogh-Moe, Acta Cryst. **9,** 951 (1956).
[10] L. Koester and E. Seyman, Atomic Data and Nuclear Data Tables **49,** 65 (1991).
[11] A. Präffcke, Diploma thesis, University Stuttgart, 1992.
[12] W. Hume-Rothery and G. V. Raynor, The Structure of Metals and Alloys, 3rd ed., Inst. Metals, London 1954.
[13] G. S. Cargill III and F. Spaepen, J. Non-Cryst. Solids **43,** 91 (1981).
[14] A. Bhatia and D. E. Thornton, Phys. Rev. **B2,** 3004 (1970).